



A QTAIM approach on poly tetrahydrothiophene molecular wire

S Palanisamy¹, P Srinivasan^{2*}, A David Stephen³ and K Selvaraju^{1*}

¹ Department of Physics, Kandaswami Kandar's College, Velur-638182, Namakkal (Dt.) India

² Department of Physics, Chikkaiah Naicker College, Erode-638004, Erode (Dt), India

³ Department of Physics, Sri Shakthi Institute of Engineering and Technology, Coimbatore-641062, India

* Corresponding authors: physicsselvaraj@gmail.com; sriniscience@gmail.com

Abstract

The present investigation of structural, charge density and electrical characteristics of Au and thiol substituted poly tetrahydrothiophene molecular wire by using quantum chemical calculations has been carried out with density functional theory (DFT). The various applied electric field ($0.00 - 0.26 \text{ V\AA}^{-1}$) altered the geometrical parameters and the corresponding electrostatic and transport properties of the molecule has been analyzed. Interestingly, the applied electric field is increased from 0 eV, the Au-S bond distance at the right terminal is faintly longer than the left end; this variation is resulted from the gold atom at the left end which practices stronger electric field when compared with at the right end of TET molecule. The variations in the atomic charges (MPA, NPA) of the molecule for the various applied electric fields have been compared. The HOMO-LUMO gap of the molecule for zero bias is 1.96eV, as the field increases this gap decrease to 1.31 eV. The ESP shows the potential difference between charges accumulated of the molecule for various applied electric field. The applied electric field polarizes the TET molecule; as a result dipole moment of the molecule rises from 2.47 to 15.33 D.

Keywords: Molecular wire; Density functional theory; HLG; ESP; Dipole moment.

1. INTRODUCTION

In the recent years, the electron transport in conjugated molecular units was facilitated by alternating single and double (or triple) bonds. Likewise, conjugated polymers like oligomers and thiophenes, exhibit the narrow HOMO-LUMO gap, around 3eV which results the delocalized π -electrons and higher electrical conductivity in the molecular wire [1]. The derivatives of α -Conjugated oligo- and poly thiophenes are favorable materials for a many usages in molecular electronic devices which includes molecular wire, molecular diode and molecular field-effect transistor [2]. Furthermore, they also provide an exciting model for realizing the electrical characteristics of conjugated molecular nano wire materials because of their distinctive conjugation structure. This study describes the electrical conductivity and the topological electron density analysis of poly tetrahydrothiophene based molecular nanowire under various applied electric field. In the electrode-molecule-electrode system, commonly, the organic molecules reveals the discrete electronic energy levels and switching of isolated heavy metal atoms at both the right and left ends, differ the electronic energy levels of the molecular nano wire. Thus, the connection between the electrode and the molecule has an important role in the electron-transport characteristics of the molecular nano wire. Additionally, this computational research article describes the outcome of external electric applied field on the thiophene molecule using thiol atom as terminal atom for applying electric field. This work discovers the electron density as well as the total energy density distribution and the influence of gold metal atom in sulphur linked tetrahydrothiophene-2-ylethyl-tetrahydrothiophene (TET) molecule (Figure. 1) for the various levels of bias applied on both the left (L-end) and right side (R-end) from QTAIM [3] via high level quantum chemical calculations.

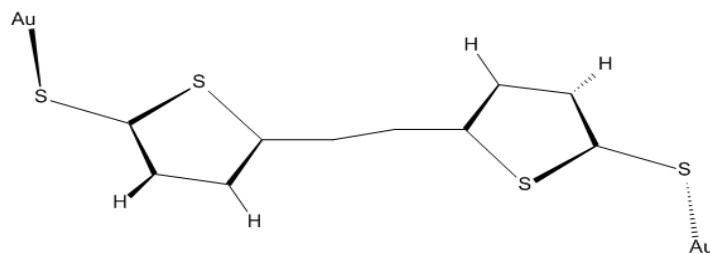


Figure. 1 The chemical structure of Au and S substituted tetrahydrothiophene-2-ylethyl-tetrahydrothiophene molecule.

2. THEORETICAL METHODOLOGY

The optimization of Au and thiol substituted TET system was carried out for the five different applied electric fields 0.05, 0.10, 0.15, 0.21 and 0.26 $\text{V}\text{\AA}^{-1}$ as positive potential on the L-end and negative field on the R-end of the TET molecule using density functional algorithm [4] computations implemented in Gaussian09 program suite [5]. The computation was performed with the B3LYP hybrid function (Becke's three parameters exchange function and Lee, Yang and Parr gradient-corrected correlation function) [6] and LANL2DZ (Los Alamos National Laboratory of Double Zeta) as basis set [7], which delivers the operative core potential and the thorough explanation of the consequence of the presence of heavy metal atoms in the molecule. Geometry optimization was carried out by incorporating the Berny algorithm. The optimization was accomplished with the threshold convergence for maximum force, 0.00045 au, root mean square (RMS) force, 0.0003 au, maximum displacement, 0.001 au and root mean square (RMS) displacement, 0.0012 au. The convergence on the density matrix of 10^{-8} and 10^{-6} for the RMS and maximum density matrix error between the iterations was requested to perform the self consistent solution of non-interactive wave function. An external dipolar field is customized to calculate the influence of voltage as part of Hamiltonian.

The topology of charge density at the bond critical point (bcp) such as electron density $\rho_{\text{bcp}}(r)$, Laplacian of electron density $\nabla^2\rho_{\text{bcp}}(r)$, bond ellipticity ϵ and the eigenvalues λ_i was computed for five different applied electric fields using EXT94b module implemented in AIMPAC suite [8]. The graphical program packages DENPROP [9] and wfn2plots [10] were used to generate 2D/3D grid for plotting Laplacian of charge density and the deformation density maps. The three dimensional surface plots of molecular orbitals (HOMO and LUMO) and molecular electrostatic potential (MESP) were posed from GVIEW package [11]. Also, the density of states (DOS) at five different levels of applied EFs was calculated from GaussSum program [12].

3. RESULTS AND DISCUSSION

3.1 Molecular Geometry

Figure 2 depicts the optimized structure of Au and S substituted TET molecular wire for the zero and higher applied electric field. TET molecular wire constitutes two thiophene five membered rings and the gold atoms are attached at right and left side of the TET molecule through sulphur atoms. As described earlier, the sulphur atom provides an outstanding link between the conjugated poly thiophene molecule and the gold atom. Commonly, the conducting molecular wires are very responsive to the applied external electric potential and the applied bias varies the geometry conformation of the molecule, which results the considerable modification in the transport properties of the molecules. Further, the bond distance variation due to the applied electric field has an important role in predicting the conductance of molecular wires. Hence, it is mandatory to relate the zero electric field confirmation of the TET molecule with the higher applied fields to realize its structural stability over the wide range of applied electric field from 0 to 0.26eV.

The C-C bond lengths of two thiophene rings and the C-C bonds which connects the thiophene rings in the molecule are 1.425 and 1.402 \AA respectively for zero electric field. But the C(5)=C(6) bond displays a less value of 1.233 \AA , which approves its double bond nature. The double bond lengths [C(1)-C(2), C(3)-C(4), C(7)-C(8) and C(9)-C(10)] were enlarged maximum by 0.009 \AA , when the field increases, unlikely, the single bond lengths [C(2)-C(3), C(4)-C(5), C(6)-C(7) and C(8)-C(9)] were decreased by same trend. The average zero field lengths of S-C bonds of the thiophene rings is ~ 1.82 \AA ; further, as the field increases, the perceived maximum deviation is 0.007 \AA . Equally, the applied electric field reformed the bond lengths of terminal S-C bonds, which are seems to be uneven on both ends. In the L-end, the bond length elongated from 1.790 to 1.797 \AA , whereas at the right end, this was shortened from 1.790 to 1.772 \AA ; however, the deviation in the L-end is marginally larger than the R-end and the maximum deviation is 0.007 \AA . Particularly, the ring S-C bond lengths are considerably elongated than the terminal S-C bonds (Table 1). The applied electric fields

show no influence over the C–H bond lengths and are nearly equal to the zero field lengths (1.084 Å). The bond lengths of Au–S bonds are found unequal under zero and non-zero field. When the applied electric field increases, the bond length at the left end is found to be decreased from 2.421 to 2.411 Å, unlikely in the R-end, the bond length rises from 2.421 to 2.462 Å; however the deviations in both left and right ends are not equal. And, for the highest applied electric field, 0.26 $\text{V}\text{\AA}^{-1}$, the deviations of 0.009 and 0.0415 Å were noticed at the right and left end of the molecule. This massive difference results from the applied field elongating the Au–S bond distance through by decreasing the S–C bond length in the wire; the bond distances of Au–S and S–C agree well previously published values [13,14]. The variation of bond lengths for zero and higher electric field of TET molecular wire is shown in the figure 3.

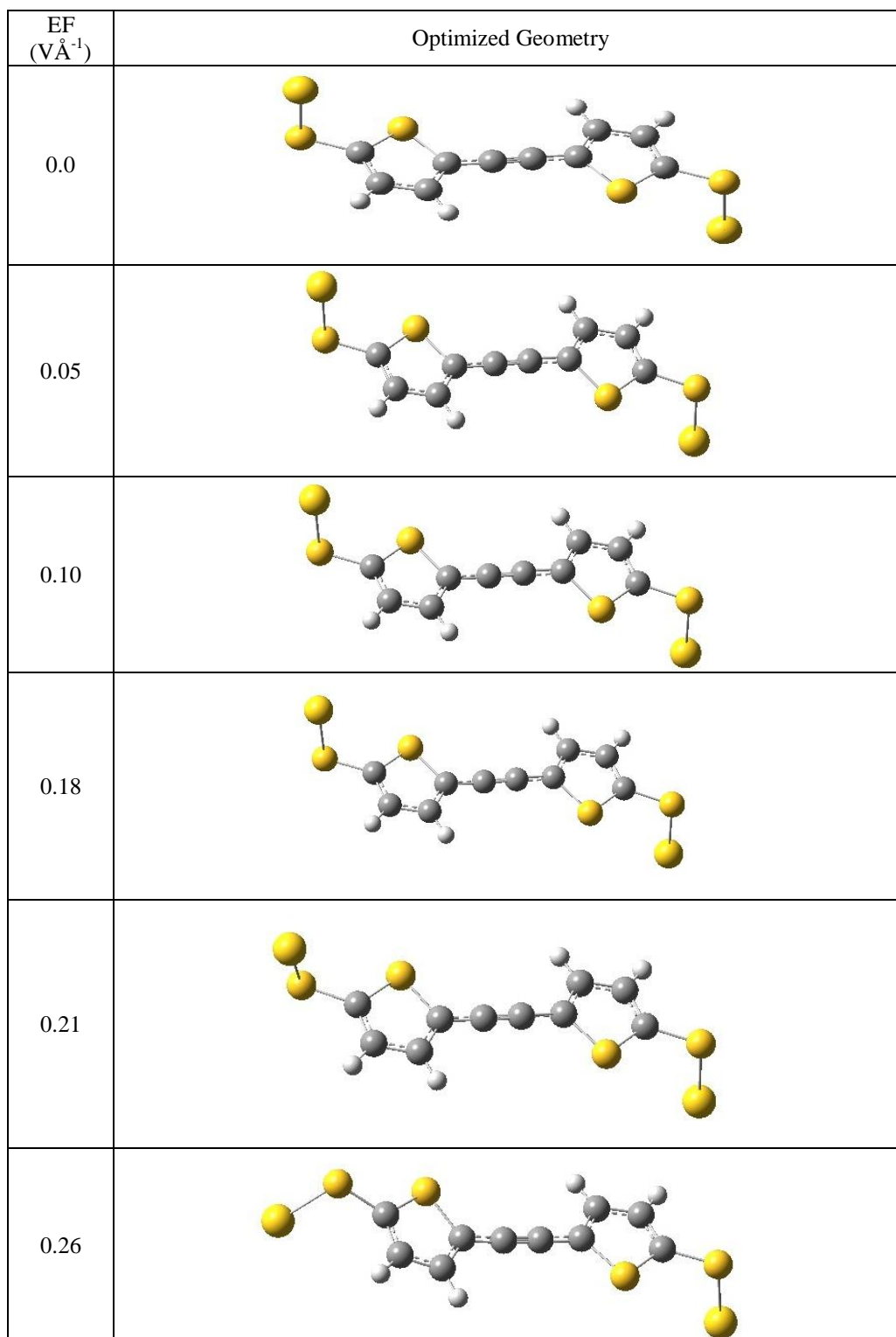


Figure. 2 Optimized geometry of Au and S substituted TET molecule for the zero and various applied EFs.

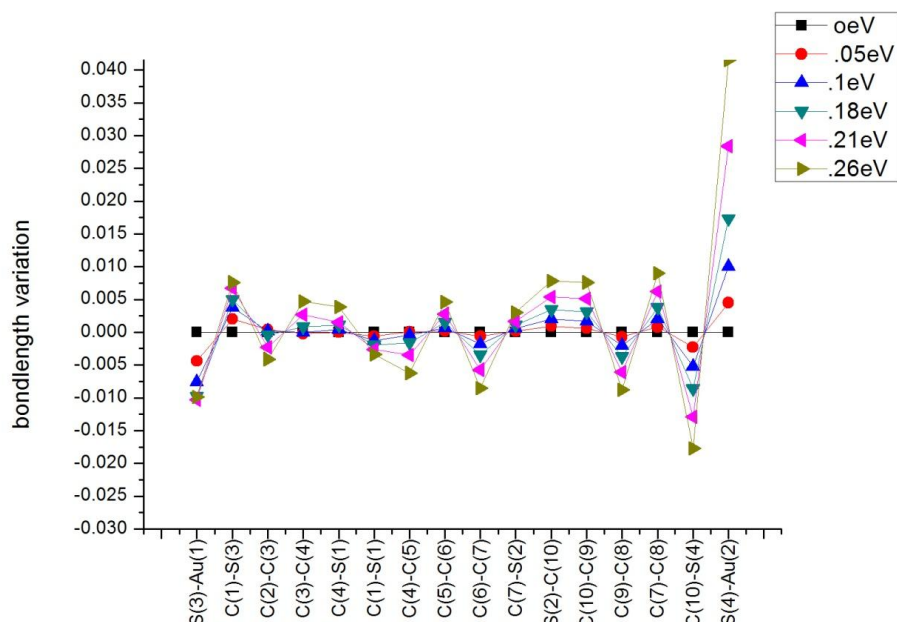


Figure. 3 Showing the bond length variation of Au and S substituted TET molecule for zero and various applied EFs.

Table. 1 Bond distance (Å) of [(2R)-5-[2-[(2S)-5-aurosulfanyl]tetrahydrothiophen-2-yl]ethyl]tetrahydrothiophen-2-yl]sulfanylgold molecule for different potential EFs ($\text{V}\text{\AA}^{-1}$).

Bonds	Applied electric field					
	0	0.05	0.1	0.18	0.21	0.26
Ring 1						
C(1)-C(2)	1.390	1.390	1.390	1.391	1.392	1.394
C(1)-S(1)	1.815	1.814	1.813	1.813	1.812	1.811
C(2)-C(3)	1.425	1.425	1.425	1.425	1.423	1.421
C(3)-C(4)	1.396	1.396	1.396	1.397	1.399	1.401
C(4)-S(1)	1.821	1.821	1.821	1.822	1.822	1.825
Ring 2						
C(7)-S(2)	1.821	1.821	1.821	1.822	1.823	1.824
C(7)-C(8)	1.396	1.397	1.398	1.400	1.402	1.405
S(2)-C(10)	1.815	1.815	1.817	1.818	1.820	1.822
C(10)-C(9)	1.390	1.391	1.392	1.394	1.396	1.398
C(9)-C(8)	1.425	1.424	1.423	1.421	1.419	1.416
Ring Connector						
C(4)-C(5)	1.402	1.402	1.402	1.400	1.399	1.396
C(5)-C(6)	1.233	1.234	1.234	1.235	1.236	1.238
C(6)-C(7)	1.402	1.401	1.400	1.399	1.396	1.394
Terminal Bonds						
S(3)-Au(1)	2.421	2.416	2.413	2.411	2.410	2.411
C(1)-S(3)	1.790	1.792	1.793	1.795	1.796	1.797
C(10)-S(4)	1.790	1.787	1.784	1.781	1.777	1.772
S(4)-Au(2)	2.421	2.425	2.431	2.438	2.449	2.462

C-H bonds						
C(2)-H(2)	1.084	1.084	1.084	1.084	1.084	1.084
C(3)-H(3)	1.084	1.084	1.084	1.084	1.084	1.085
C(8)-H(8)	1.084	1.084	1.084	1.084	1.084	1.084
C(9)-H(9)	1.084	1.084	1.084	1.084	1.084	1.084

Further, the applied fields make no significant variations the bond angles of the molecule and are nearly equal to the computed angles for the zero electric field. However, the higher electric field made a substantial variation in the bond angles of the terminal, S–C–S and Au–S–C bonds. At the left end, the zero electric field bond angle for the S(3)–C(1)–S(1) bond is 121.8°, when the field increases to 0.26 VÅ⁻¹, this angle was marginally decreased to ~119.9°; whereas at the right end, the bond angle C(10)–S(4)–Au(2) steadily increases from ~121.82 to ~122.26°. The angle deviation about C(1) may be resulted from the rotation of S(1)–C(1) bond at the left end. The terminal C–C–S bond angles for the zero field in the left edge is 127.22° and, this value was slightly get shifted to 128.84° when the field increases to 0.26 VÅ⁻¹, likely at the right region, the angle seems increasing from 127.22° to 127.42°. When the field increases, terminal angle C–S–Au bonds present at the both right and left ends increases; in which, the maximum deviation observed at the left end is 0.7°, while the variation at the right end is 2.12°. The applied higher fields made no influence over angular variations in C–C–C and C–C–H bonds, as the variation is very small. The complete bond angles of TET molecule for the zero and non-zero fields are listed in Table 2.

Table 2 Bond angles (°) of [(2R)-5-[2-[(2S)-5-aurosulfanyltetrahydrothiophen-2-yl]ethyl]tetrahydrothiophen-2-yl]sulfanylgold molecule for different potential EFs (VÅ⁻¹).

Bonds	Applied electric field					
	0	0.05	0.1	0.18	0.21	0.26
Ring 1						
C(2)-C(1)-S(1)	110.83	110.86	110.90	110.92	110.91	110.89
C(1)-C(2)-C(3)	114.43	114.40	114.39	114.40	114.40	114.43
C(2)-C(3)-C(4)	114.16	114.15	114.15	114.15	114.20	114.29
C(3)-C(4)-S(1)	110.54	110.56	110.55	110.51	110.43	110.26
C(1)-S(1)-C(4)	90.04	90.03	90.02	90.02	90.06	90.11
Ring 2						
S(2)-C(7)-C(8)	110.54	110.51	110.47	110.41	110.33	110.21
C(7)-S(2)-C(10)	90.04	90.06	90.09	90.13	90.18	90.25
S(2)-C(10)-C(9)	110.83	110.77	110.69	110.59	110.45	110.28
C(10)-C(9)-C(8)	114.43	114.47	114.53	114.62	114.73	114.86
C(7)-C(8)-C(9)	114.16	114.18	114.21	114.25	114.31	114.39
Ring Connector						
C(3)-C(4)-C(5)	128.34	128.38	128.42	128.46	128.58	128.82
S(1)-C(4)-C(5)	121.11	121.06	121.02	121.01	120.96	120.90
C(6)-C(7)-S(2)	121.11	121.20	121.33	121.52	121.80	122.05
C(6)-C(7)-C(8)	128.35	128.29	128.20	128.07	127.87	127.71
Terminal bond						
C(1)-S(3)-Au(1)	104.30	104.64	104.81	105.02	104.90	104.99
C(2)-C(1)-S(3)	127.22	127.21	127.15	127.06	128.20	128.84
S(1)-C(1)-S(3)	121.82	121.72	121.67	121.67	120.56	119.95
S(2)-C(10)-S(4)	121.82	121.89	121.98	122.07	122.17	122.26
C(9)-C(10)-S(4)	127.22	127.26	127.29	127.31	127.36	127.42
C(10)-S(4)-Au(2)	104.30	104.14	104.28	104.59	105.25	106.42

C-C-H Bonds

C(1)-C(2)-H(2)	121.82	121.81	121.77	121.72	121.70	121.72
C(3)-C(2)-H(2)	123.75	123.79	123.84	123.88	123.89	123.85
C(2)-C(3)-H(3)	123.80	123.75	123.71	123.67	123.63	123.58
C(4)-C(3)-H(3)	122.04	122.10	122.14	122.17	122.16	122.13
C(10)-C(9)-H(9)	121.82	121.82	121.79	121.75	121.68	121.60
C(8)-C(9)-H(9)	123.75	123.71	123.67	123.63	123.59	123.54
C(7)-C(8)-H(8)	122.04	121.97	121.89	121.79	121.68	121.56
C(9)-C(8)-H(8)	123.80	123.84	123.90	123.95	124.01	124.06

On compared with the L-end and R-end bonds the applied electric field leads slight twist in the C-C-C bonds of the five membered rings as well as the spine bonds of the TET molecule, maximum variations in the bond twist at the zero and non-zero fields for the C-C-C-C bond (ring 1) is 0.3° where the bond displays an high dihedral angle of 0.428/-0.428° at zero applied electric field and for the maximum electric field, 0.21 VÅ⁻¹, the dihedral angle shifted to a value of -0.269/-0.713°. The significant variations in the torsion angles are prominent in the case of C-C-C-C bond at the ring linker where the dihedral angle is varied from -179.927° for the zero field to 178.366° when the applied field increases to 0.26 VÅ⁻¹. The same trend is noticed for left end of the connector with C(5)-C(4)-S(1)-C(1), where the dihedral angle is varied from 179.939° [for 0 VÅ⁻¹] to -177.281° [for 0.26 VÅ⁻¹]. The dihedral angles of Au-S-C-C bonds in left and right ends are 98.4 and -98.8° respectively for the zero field, when the field increases, the respective observed angles are getting diversified by 5° in right end and 180° in left end respectively. The differences in the L-end terminal have been considerably diversified, which shows that the left end group is highly reactive to the positive potential than the negative potential. However, there is no substantial difference detected in the C-C-C-H bonds of the TET molecular wire for the different bias [Table 3]. The exact structural variation of TET molecule for zero and the applied fields was depicted in the Figure. 2. On the whole, comparatively the left and right end groups seem more respondent to the applied electric field.

Table 3 Torsion angles (°) of Au and S substituted [(2R)-5-[2-[(2S)-5-auriosulfanyltetrahydrothiophen-2-yl]ethyl]tetrahydrothiophen-2-yl]sulfanylgold molecule for different potential EFs (VÅ⁻¹).

Bonds	Applied electric field					
	0	0.05	0.1	0.18	0.21	0.26
Ring 1						
S(1)-C(1)-C(2)-C(3)	-0.198	-0.239	-0.244	-0.249	-0.319	0.707
C(2)-C(1)-S(1)-C(4)	-0.044	0.088	0.150	0.185	0.646	-1.098
C(3)-C(4)-S(1)-C(1)	0.274	0.081	-0.022	-0.081	-0.825	1.235
C(1)-C(2)-C(3)-C(4)	0.428	0.313	0.235	0.193	-0.337	0.269
Ring Connector						
C(5)-C(4)-S(1)-C(1)	179.939	179.149	178.701	178.363	177.199	-177.281
C(3)-C(4)-C(7)-S(2)	-0.386	0.715	0.053	-1.300	-7.433	-9.725
C(3)-C(4)-C(7)-C(8)	-179.993	179.642	178.226	176.559	171.086	173.743
S(1)-C(4)-C(7)-S(2)	179.994	-177.313	-177.055	-177.773	176.496	167.101
S(1)-C(4)-C(7)-C(8)	0.387	1.614	1.118	0.085	-4.984	-9.432
C(6)-C(7)-S(2)-C(10)	-179.934	179.478	179.279	179.312	179.884	-177.946
C(6)-C(7)-C(8)-C(9)	-179.927	-179.264	-178.991	-178.955	-179.461	178.366
Ring 2						
C(8)-C(7)-S(2)-C(10)	-0.273	-0.371	-0.358	-0.285	-0.025	-177.946
C(7)-S(2)-C(10)-C(9)	0.042	0.088	0.023	-0.100	-0.391	-0.992
S(2)-C(10)-C(9)-C(8)	0.200	0.218	0.322	0.468	0.728	1.159
C(10)-C(9)-C(8)-C(7)	-0.428	-0.527	-0.624	-0.718	-0.779	-0.713
Terminal Bonds						
S(3)-C(1)-C(2)-C(3)	175.634	174.530	173.723	172.974	173.030	-172.745

S(3)-C(1)-S(1)-C(4)	-176.138	-175.015	-174.201	-173.462	-173.286	173.019
C(2)-C(1)-S(3)-Au(1)	98.843	98.626	98.937	99.437	83.700	-77.234
S(1)-C(1)-S(3)-Au(1)	-85.742	-87.122	-87.689	-88.005	-103.518	109.829
S(4)-C(10)-C(9)-C(8)	-175.630	-176.573	-177.138	-177.531	-177.549	-176.784
C(7)-S(2)-C(10)-S(4)	176.134	177.080	177.640	178.022	177.991	177.076
S(2)-C(10)-S(4)-Au(2)	0.200	85.312	85.281	85.524	86.644	88.787
C(9)-C(10)-S(4)-Au(2)	-98.842	-98.223	-97.521	-96.687	-95.263	-93.496

3.2 Electron density Analysis

The link between the topology of charge density at the bond critical points and the chemical concepts can be well calculated from QTAIM [15]. The bond topological parameters at bcp of TET molecular wire for different electric potential were listed in Table 4. The QTAIM analysis is carried out for bond critical point (3,-1) for all bonds of the TET molecule, approves the existence of chemical interaction between the two atoms. In more specific, the Au-S bond embraces, the gold and sulphur interaction is not a covalent type. The bond topological exploration of the molecule discloses that the Au-S bonds reveals a positive Laplacian of electron density $\nabla^2\rho(r)$, directs the presence of *non-covalent* interaction between the metal and the thiol atoms i.e. the non-covalent interaction. The zero field electron density [$\rho_{\text{bcp}}(r)$] at the bond critical point of ring C-C bonds ranges from 1.86 to 1.97 $\text{e}\text{\AA}^{-3}$; while for the applied electric field, these density values differs marginally, the maximum deviation is 0.031 $\text{e}\text{\AA}^{-3}$. Similarly, the C-C bonds connecting the rings are ranging from $\sim 1.88 \text{e}\text{\AA}^{-3}$ to 2.46 $\text{e}\text{\AA}^{-3}$ for the zero field electron density $\rho_{\text{bcp}}(r)$, but the C(5)=C(6) which connects the thiophene rings displays a higher electron density (2.46 $\text{e}\text{\AA}^{-3}$) and are insensitive to the external applied electric potential. The S-C bond density is $\sim 1.06 \text{e}\text{\AA}^{-3}$ for the zero bias and for the higher electric field, the density seems slightly falls to 1.08 $\text{e}\text{\AA}^{-3}$. Remarkably, the less value of S-C bond density directs that the charges are migrated away from the inter-nuclear axis, which sanctions its predominant π -bond character which was agreed well from the bond ellipticity and Laplacian of electron density.

The Au-S bond electron density is $\sim 0.5 \text{e}\text{\AA}^{-3}$ at zero electric field, while for the higher electric field, the density rises from 0.503 to 0.512 $\text{e}\text{\AA}^{-3}$ in the left end, unlikely at the right end it declines from 0.503 to 0.466 $\text{e}\text{\AA}^{-3}$; however, the difference is found to be insignificant. The C-H bond electron density is $\sim 1.79 \text{e}\text{\AA}^{-3}$, which diverges marginally as the field value gets increased. The influence of electric potential in the TET molecule is very less as the bond densities of the molecule is not much altered. Comparatively, the dissimilarities are small for the applied electric field and are noted to be systematic (Table 4). The charge accumulation or exhaustion of bonds was well recognized from the Laplacian of electron density [$\nabla^2\rho_{\text{bcp}}(r)$] at the bcp. In this investigation, the Laplacian of electron density at the bond critical point of the bonds in the TET molecule has been noted for the applied external electric field. Table 5 shows the predicted Laplacian of electron density for five levels of applied electric field. Figure. 4 displays the Laplacian of electron density for the zero and non-zero potential ($\text{V}\text{\AA}^{-1}$).

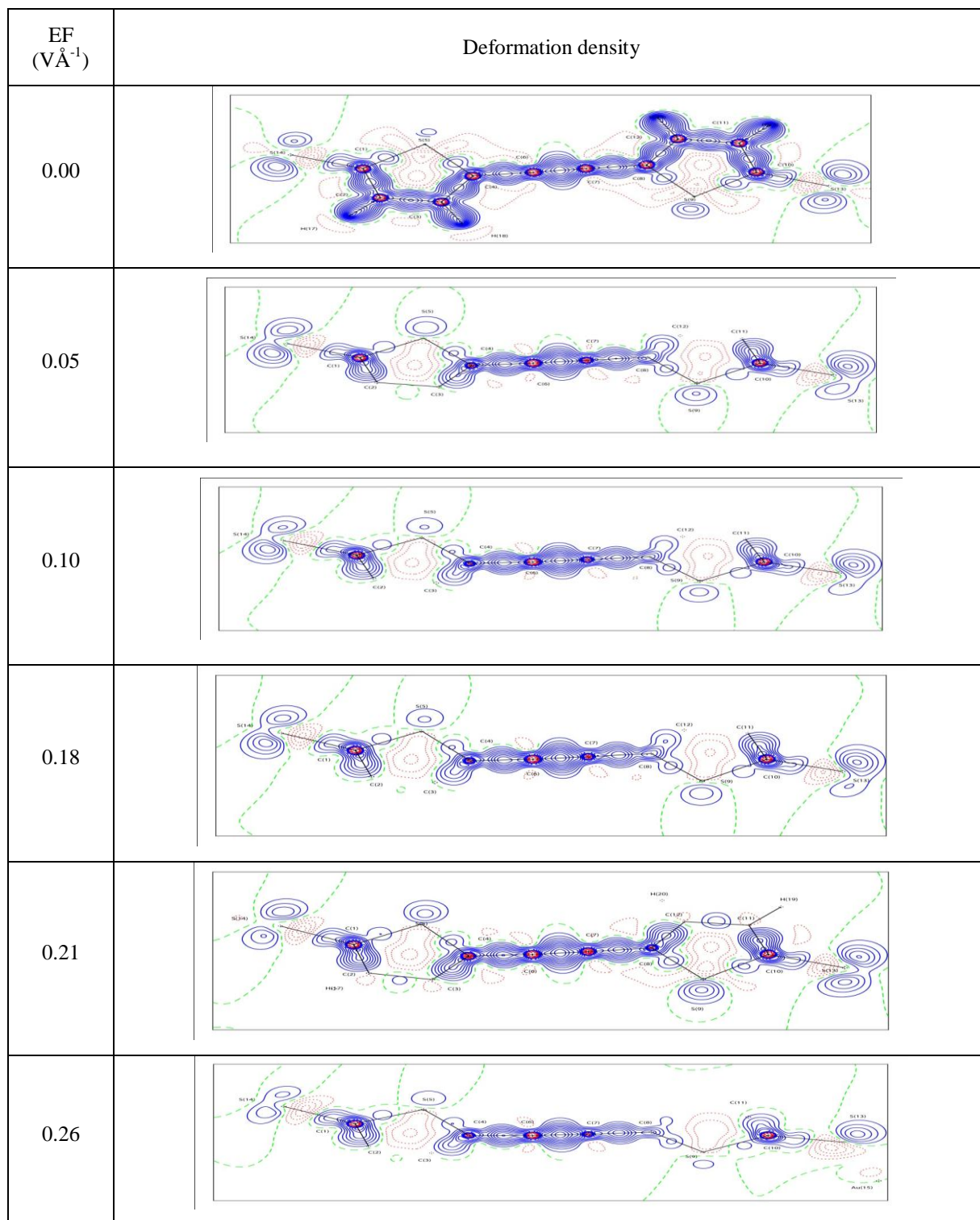


Table 4 Electron density $\rho_{\text{bcp}}(r)$ ($\text{e}\text{\AA}^{-3}$) values of Au and S substituted [(2R)-5-[2-[(2S)-5-auriosulfanyltetrahydrothiophen-2-yl]ethyl]tetrahydrothiophen-2-yl]sulfanylgold molecule for different potential EFs ($\text{V}\text{\AA}^{-1}$).

Bonds	Applied electric field					
	0	0.05	0.1	0.18	0.21	0.26
Ring 1						
C(1)-C(2)	1.972	1.973	1.973	1.971	1.967	1.960
C(3)-C(2)	1.862	1.861	1.862	1.864	1.871	1.877
C(4)-C(3)	1.95	1.950	1.95	1.947	1.940	1.933
C(1)-S(1)	1.069	1.071	1.072	1.073	1.075	1.076
C(4)-S(1)	1.056	1.056	1.055	1.053	1.052	1.048
Ring Connector						
C(5)-C(4)	1.885	1.884	1.885	1.888	1.894	1.902
C(6)-C(5)	2.465	2.465	2.463	2.46	2.456	2.449
C(7)-C(6)	1.886	1.888	1.893	1.899	1.907	1.917
Ring 2						
C(8)-C(7)	1.95	1.943	1.943	1.937	1.929	1.92
C(9)-C(8)	1.862	1.869	1.869	1.875	1.883	1.893
C(9)-C(10)	1.972	1.966	1.966	1.961	1.954	1.946
C(7) S(2)	1.056	1.056	1.056	1.055	1.054	1.052
C(10) S(2)	1.069	1.067	1.065	1.062	1.059	1.054
C-H Bonds						
H(2)-C(2)	1.799	1.800	1.801	1.803	1.803	1.803
C(9)-H(9)	1.799	1.799	1.798	1.797	1.796	1.796
C(3)-H(3)	1.796	1.795	1.795	1.796	1.796	1.796
H(8)-C(8)	1.796	1.796	1.796	1.796	1.797	1.797
Terminal Bonds						
C(1)-S3	1.069	1.064	1.06	1.057	1.052	1.048
S(3)-Au(1)	0.503	0.507	0.509	0.511	0.511	0.512
C(10)-S(4)	1.069	1.073	1.078	1.083	1.089	0.219
S(4)-Au(2)	0.503	0.499	0.494	0.487	0.477	0.466

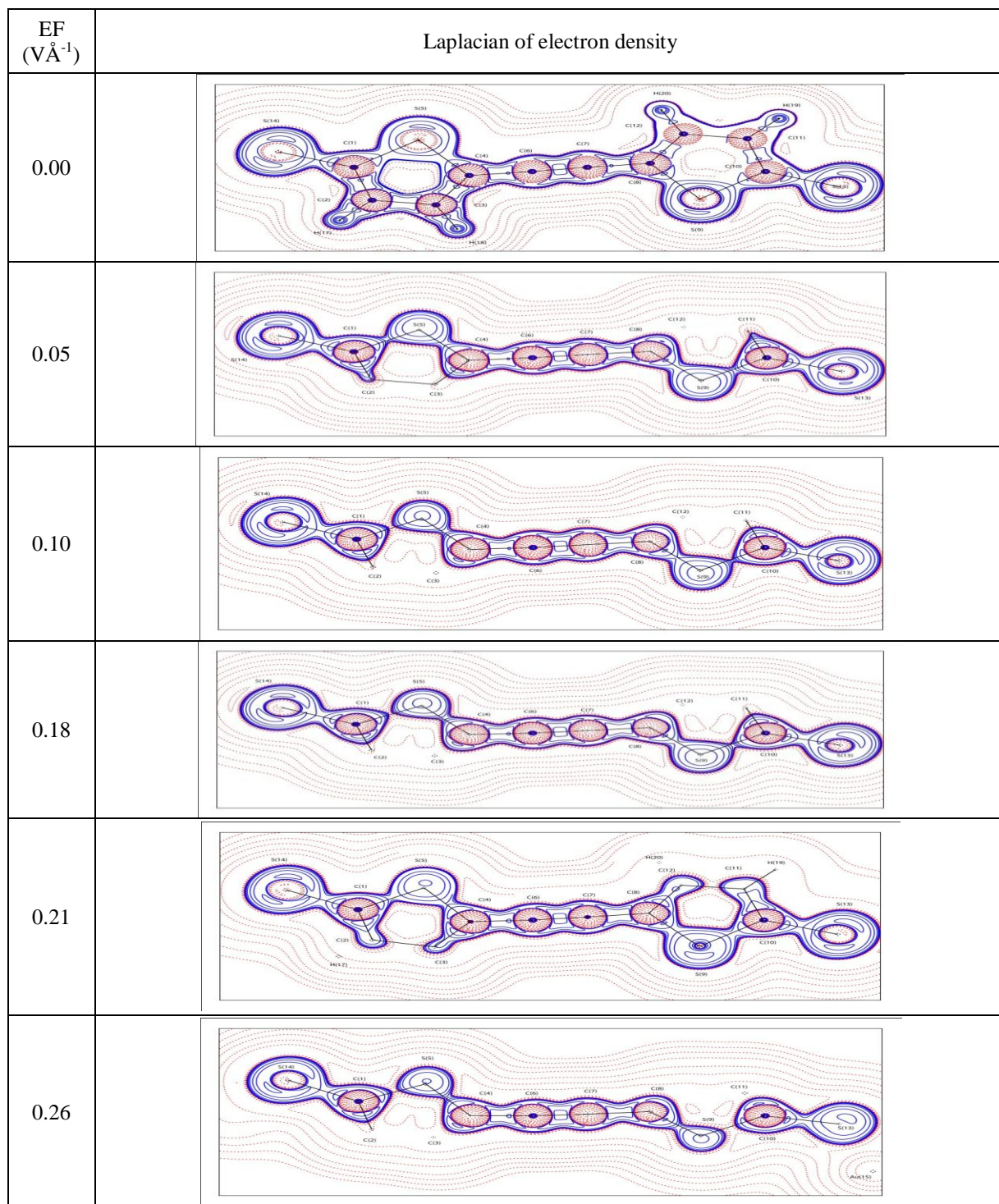


Figure. 5 Laplacian of electron density maps of the TET molecule for different potential EFs ($\text{V}\text{\AA}^{-1}$).

The calculated Laplacian of electron density for the ring C–C bonds are ranging from $-16.8 \text{ e}\text{\AA}^{-5}$ to $-18.2 \text{ e}\text{\AA}^{-5}$ for the zero electric field; while for the high electric field, the $\nabla^2\rho_{\text{bcp}}(\text{r})$ values are found slightly less negative shows that the charges of these bonds are faintly getting depleted. Among the ring connectors, the covalent character of C(6)=C(5) bond is found to be high as the laplacian value at the bond critical point is $\sim 24.5 \text{ e}\text{\AA}^{-5}$ which are not suggestively vary by the external applied electric field. It is renowned that the laplacian of C(7)-C(6) and C(4)-C(5) bonds becoming little negative which ranges from -17.7 to $-18.3 \text{ e}\text{\AA}^{-5}$. The Laplacian of electron density for the C–H bonds is $\sim -21 \text{ e}\text{\AA}^{-5}$ for the zero field, this high negative value displays the charge accumulation, and the high electric field modify this charge concentration in a feeble amount. The S–C bond charges are found to be less accumulated for the zero field and its respective $\nabla^2\rho_{\text{bcp}}(\text{r})$ value is $\sim -4.90 \text{ e}\text{\AA}^{-5}$; this value was found to decreases to $\sim -5.6 \text{ e}\text{\AA}^{-5}$ when field value is increased from 0 eV; however, the variations in Laplacian values specifies that the charges at the left end are marginally more depleted than the right end. The Laplacian of Au–S bond is $3.018 \text{ e}\text{\AA}^{-5}$ for the zero field, when the field increases, this value sharply increases to $3.269 \text{ e}\text{\AA}^{-5}$ at the L-end but at the right end it decreases to $2.952 \text{ e}\text{\AA}^{-5}$. On the whole, the Laplacian of electron density distribution in the Au substituted TET molecular wire (Au–S–molecule–S–Au), exposes that the applied electric potential depletes the electron distribution at the bond critical point of C–C bonds, while this scenario is found enhanced in the left and right end bonds, precisely it is high at the right end.

Table 5 Laplacian of electron density $\nabla^2\rho_{\text{bcp}}(\text{r})$ ($\text{e}\text{\AA}^{-5}$) values of Au and S substituted [(2R)-5-[2-[(2S)-5-auriosulfanyltetrahydrothiophen-2-yl]ethyl]tetrahydrothiophen-2-yl]sulfanylgold molecule for different potential EFs ($\text{V}\text{\AA}^{-1}$).

Bonds	Applied electric field					
	0	0.05	0.1	0.18	0.21	0.26
Ring 1						
C(1)-C(2)	-18.2	-18.2	-18.2	-18.2	-18.1	-18.0
C(3)-C(2)	-16.8	-16.8	-16.8	-16.9	-17.0	-17.1
C(4)-C(3)	-17.9	-17.9	-17.9	-17.9	-17.7	-17.7
C(1)-S(1)	-4.484	-4.494	-4.505	-4.513	-4.533	-4.558
C(4)-S(1)	-4.487	-4.491	-4.48	-4.462	-4.451	-4.383
Ring Connector						
C(5)-C(4)	-17.7	-17.7	-17.7	-17.7	-17.8	-17.8
C(6)-C(5)	-24.5	-24.5	-24.5	-24.5	-24.5	-24.4
C(7)-C(6)	-17.7	-18.0	-17.9	-18.0	-18.1	-18.3
Ring 2						
C(8)-C(7)	-17.9	-17.8	-17.8	-17.7	-17.5	-17.4
C(9)-C(8)	-16.8	-16.9	-17.0	-17.1	-17.2	-17.4
C(9)-C(10)	-18.2	-18.1	-18.1	-18.0	-17.9	-17.7
C(7) S(2)	-4.487	-4.479	-4.466	-4.449	-4.427	-4.381
C(10) S(2)	-4.484	-4.466	-4.439	-4.402	-4.345	-4.276
C-H Bonds						
H(2)-C(2)	-21.2	-21.2	-21.3	-21.3	-21.4	-21.4
C(9)-H(9)	-21.2	-21.1	-21.1	-21.0	-21.0	-21.0
C(3)-H(3)	-21.0	-21.0	-21.0	-21.0	-21.0	-21.0
H(8)-C(8)	-21.0	-21.0	-21.0	-21.0	-21.0	-21.1
Terminal Bonds						
C(1)-S3	-5.733	-5.665	-5.614	-5.601	-5.585	-5.624
S(3)-Au(1)	3.018	3.05	3.081	3.115	3.15	3.269
C(10)-S(4)	-5.732	-5.822	-5.957	-6.152	-6.564	5.025
S(4)-Au(2)	3.018	2.996	2.981	2.969	2.956	2.952

The bond ellipticity $\varepsilon = (\lambda_1/\lambda_2)-1$, can be calculated to determine the anisotropy of charge density distribution at the bond critical point of molecules, where λ_1 and λ_2 are the negative eigen values of Hessian matrix [16]. The high value of ellipticity denotes the wide anisotropy of bonding density and hence strong

deviations from σ -type bond nature. The average value of ellipticity for C–C bonds is found less (i.e) 0.2, except for the C(3)-C(2) of ring 1 and C(9)-C(8) of ring 2, showing the ellipticity value around 0.12 and progressively increases with field increases. The ellipticity of S–C bond at both right [0.117 to 0.107] and left ends [0.182 to 0.115] of the wire decreased gradually. On relating with Au–S bonds, the ellipticity value at left end region is found increasing from 0.182 to 0.226 with electric field where at the right end region the field is found to be less effective (Table 6) which depicts that the densities are found to be highly anisotropy at left end region. Further, the C–H bonds exhibit very low ellipticity value ranges from 0.008 to 0.014. The predicted values of ellipticity of the TET molecule for various applied electric field are listed in Table 6.

Table 6 Bond ellipticity of Au and S substituted [(2R)-5-[2-[(2S)-5-aurosulfanyltetrahydrothiophen-2-yl]ethyl]tetrahydrothiophen-2-yl]sulfanylgold molecule for the zero and various applied EFs.

Bonds	Applied electric field					
	0	0.05	0.1	0.18	0.21	0.26
Ring 1						
C(1)-C(2)	0.197	0.198	0.197	0.194	0.19	0.185
C(3)-C(2)	0.123	0.124	0.123	0.124	0.126	0.129
C(4)-C(3)	0.194	0.195	0.194	0.191	0.186	0.181
C(1)-S(1)	0.219	0.219	0.219	0.218	0.218	0.219
C(4)-S(1)	0.222	0.222	0.222	0.222	0.221	0.219
Ring Connector						
C(5)-C(4)	0.083	0.081	0.083	0.086	0.09	0.096
C(6)-C(5)	0.052	0.05	0.052	0.055	0.06	0.066
C(7)-C(6)	0.081	0.08	0.081	0.083	0.086	0.089
Ring 2						
C(8)-C(7)	0.192	0.194	0.192	0.189	0.184	0.178
C(9)-C(8)	0.129	0.126	0.129	0.131	0.135	0.138
C(9)-C(10)	0.195	0.197	0.195	0.193	0.189	0.184
C(7)-S(2)	0.222	0.221	0.221	0.22	0.219	0.218
C(10)-S(2)	0.219	0.22	0.219	0.219	0.218	0.216
C-H Bonds						
H(2)-C(2)	0.008	0.009	0.009	0.009	0.01	0.011
C(9)-H(9)	0.008	0.008	0.007	0.007	0.006	0.006
C(3)-H(3)	0.011	0.011	0.01	0.009	0.008	0.006
H(8)-C(8)	0.011	0.012	0.013	0.013	0.014	0.014
Terminal Bonds						
C(1)-S3	0.117	0.117	0.116	0.115	0.113	0.107
S(3)-Au(1)	0.182	0.188	0.195	0.205	0.214	0.226
C(10)-S(4)	0.182	0.178	0.177	0.18	0.202	0.115
S(4)-Au(2)	0.117	0.118	0.118	0.117	0.117	0.226

3.4 Energy density distribution

The essential and satisfactory conditions for chemical bonding in the molecules can be gained from both energy distribution as well as electrostatic potential of chemical bonds [17]. And so, the energy density distribution has been computed for the TET molecule, which is strongly associated to the Laplacian of electron density. The positive $\nabla^2\rho_{\text{bcp}}(\mathbf{r})$ leads the dominant of the kinetic energy density, which results the depletion of bond charge at the bond critical point; whereas the negative Laplacian denotes the dominance of potential energy density, and the accumulation of charges. The total energy density $H(\mathbf{r})$ in the bonding region can be expressed as $H(\mathbf{r}) = G(\mathbf{r})$ [Kinetic energy density] + $V(\mathbf{r})$ [Potential energy density]. In the current analysis, the $G(\mathbf{r})$ is positive, $V(\mathbf{r})$ is negative and the total energy density $H(\mathbf{r})$ is negative, it is obvious that $V(\mathbf{r})$ is always dominates for all cases. The total energy density distribution of the TET molecular wire for applied electric

field from 0 to 0.26eV is shown in Fig. 6. Comparatively, the expected zero field energy density $H(r)$ for the C–C bond of the thiophene ring seems high, $\sim -1.92 \text{ HA}^{-3}$ when compared with the other bonds. When the applied electric field rises this value was found to decreased slightly [$\sim -1.90 \text{ HA}^{-3}$]. From the table 7, it was found that the energy density of the ring linker, C(6)-C(5) shows the high value of -3.205 HA^{-3} and diluted to -3.169 HA^{-3} with increase of applied electric field.

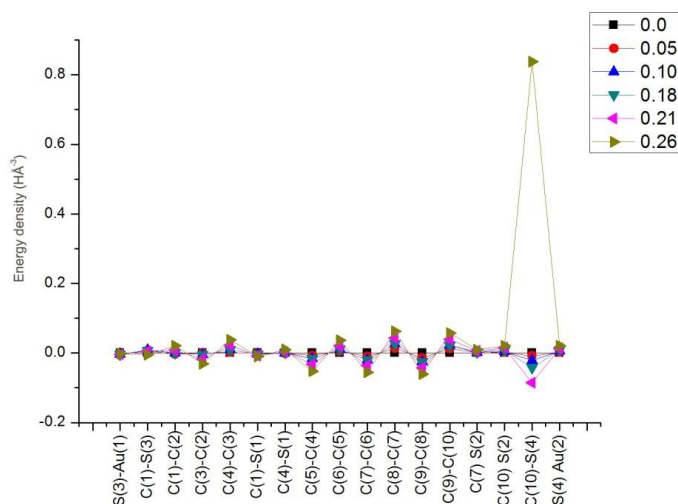


Figure. 6 Showing the energy density variation of Au and S substituted [(2R)-5-[2-[(2S)-5-auriosulfanyltetrahydrothiophen-2-yl]ethyl]tetrahydrothiophen-2-yl]sulfanylgold molecule for the different potential EFs.

Table 7 Bond energy density (HA^{-3}) distribution of Au and S substituted [(2R)-5-[2-[(2S)-5-auriosulfanyltetrahydrothiophen-2-yl]ethyl]tetrahydrothiophen-2-yl]sulfanylgold for the zero and various applied EFs ($\text{V}\text{\AA}^{-1}$).

Bonds	Applied electric field					
	0	0.05	0.01	0.18	0.21	0.26
Ring 1						
C(1)-C(2)	-2.008	-2.011	-2.007	-2.007	-2	-1.987
C(3)-C(2)	-1.772	-1.772	-1.777	-1.777	-1.789	-1.802
C(4)-C(3)	-1.974	-1.972	-1.965	-1.965	-1.951	-1.936
C(1)-S(1)	-0.668	-0.669	-0.671	-0.672	-0.675	-0.678
C(4)-S(1)	-0.662	-0.662	-0.661	-0.66	-0.659	-0.652
Ring Connector						
C(5)-C(4)	-1.856	-1.863	-1.872	-1.872	-1.888	-1.908
C(6)-C(5)	-3.205	-3.2	-3.194	-3.194	-3.184	-3.169
C(7)-C(6)	-1.857	-1.867	-1.877	-1.877	-1.893	-1.912
Ring 2						
C(8)-C(7)	-1.974	-1.96	-1.948	-1.948	-1.931	-1.911
C(9)-C(8)	-1.772	-1.786	-1.797	-1.797	-1.814	-1.833
C(9)-C(10)	-2.007	-1.994	-1.984	-1.984	-1.968	-1.95
C(7) S(2)	-0.661	-0.66	-0.659	-0.658	-0.655	-0.652
C(10) S(2)	-0.668	-0.666	-0.664	-0.66	-0.653	-0.647
C-H Bond						
H(2)-C(2)	-1.753	-1.757	-1.759	-1.763	-1.764	-1.765
C(9)-H(9)	-1.753	-1.751	-1.749	-1.748	-1.746	-1.744
C(3)-H(3)	-1.745	-1.744	-1.744	-1.744	-1.745	-1.745
H(8)-C(8)	-1.745	-1.745	-1.746	-1.747	-1.749	-1.75

Terminal Bonds

S(3)-Au(1)	-0.145	-0.147	-0.148	-0.149	-0.149	-0.147
C(1)-S(3)	-0.809	-0.803	-0.801	-0.802	-0.804	-0.814
C(10)-S(4)	-0.809	-0.817	-0.83	-0.851	-0.894	0.029
S(4) Au(2)	-0.145	-0.143	-0.139	-0.136	-0.131	-0.124

The average energy density of C–H bond is -1.7 \AA^{-3} for the zero field, and there is no significant difference noted when the field increases. In the terminal regions, the energy density distribution of the bonds, Au–S and S–C are considerably less negative when compared with the other bonds in the thiophene molecule; these small variations are accredited to the characteristics of the bonds. Interestingly, when the electric field is applied, the opposite variation is noticed between both types of bonds. The total energy density $H(r)$ variation for S–C bonds is found to be uneven and ranges from -0.809 to -0.814 \AA^{-3} in the left end, when the field is increased from 0 eV to 0.21 eV , but in the right end the even variation is noticed. The total bond energy density of Au–S bond increases from -0.145 to -0.149 \AA^{-3} , while the same at the right end decreases from -0.145 to -0.124 \AA^{-3} , when the field increases from 0 to 0.26 eV . The energy density graph for applied electric field [0 to 0.26 eV] is depicted in figure 6.

4. ATOMIC CHARGES

The molecular chemical reactivity, electrostatic potential and intermolecular interactions can be well described from the point charge distribution [18]. MPA, Mulliken population analysis [19] and NPA, Natural population analysis [20] schemes are the recommended methods proposed for the calculation of atomic charges to define the electrostatic interactions precisely. Mulliken population analysis is *not* trustworthy as they are not reliable with electrostatic Poisson equation. Further, the numerous studies reported that MK method provides the finest values agreeing the electrostatic criteria. As expected, both the charge schemes compute the negative charges for all carbon atoms in the TET molecule excluding for the C6 and C5 atoms in the bridging region. The carbon atom charges from MPA algorithm differ [ranges from -0.047 to -0.482 e] with the increase of electric field. And for the hydrogen atoms, it ranges from 0.240 e to 0.276 and little variations are noted except H(9) when the electric field is increased. The positive MPA charge is observed for S(1) atom, with the field increases, the MPA charges for sulphur atom increase from 0.283 to 0.296 e ; unlikely, the charges of S(2) atom decrease from 0.283 to 0.266 e . The MPA charge of Au atom at the left end differs from -0.037 to 0.122 e , the opposite trend was observed for the Au atom present at the R-end where the values differ from -0.037 to -0.182 e .

The NPA charge for all the carbon atoms are found nearly negative but for the carbon atoms in the connector region, it is slightly positive. Unlike MPA charges, the NPA charges for hydrogen atoms are found less, $\sim 0.24 \text{ e}$; further, and the charges are same irrespective of the fields. The NPA charge of S(1) atom seems positive and varies from 0.407 to 0.422 e , but the charge of S(2) atom decreases from 0.407 to 0.388 e . The charge of Au-atom at the left end increases progressively from 0.215 to 0.391 e with the field, whereas the opposite trend was happened at the right end as the charges were decreased from 0.215 to 0.045 e . Overall, the charges for the terminal atoms are highly sensitive to the applied electric field. The complete variation of atomic charges of all the atoms were listed in Table 8.

Table 8 Atomic charges (e) of Au and S TET molecule for the different potential EFs (V\AA^{-1}).

Atoms	Applied electric field					
	0	0.05	0.1	0.18	0.21	0.26
C(1)	-0.476	-0.475	-0.474	-0.473	-0.485	-0.482
	-0.374	-0.37	-0.365	-0.36	-0.353	-0.343
C(2)	-0.065	-0.064	-0.064	-0.063	-0.048	-0.047
	-0.231	-0.233	-0.235	-0.236	-0.239	-0.244
C(3)	-0.273	-0.272	-0.27	-0.267	-0.265	-0.262
	-0.202	-0.197	-0.192	-0.186	-0.18	-0.173
C(4)	-0.159	-0.162	-0.165	-0.168	-0.17	-0.173
	-0.226	-0.233	-0.24	-0.246	-0.252	-0.256
C(5)	0.077	0.082	0.088	0.093	0.099	0.104
	0.005	0.015	0.025	0.035	0.044	0.052
C(6)	0.077	0.071	0.067	0.063	0.062	0.06
	0.005	-0.005	-0.014	-0.022	-0.028	-0.033
C(7)	-0.159	-0.157	-0.154	-0.152	-0.151	-0.15
	-0.226	-0.219	-0.213	-0.206	-0.2	-0.195
C(8)	-0.273	-0.274	-0.275	-0.276	-0.275	-0.274
	-0.202	-0.206	-0.209	-0.212	-0.214	-0.215
C(9)	-0.065	-0.065	-0.065	-0.064	-0.063	-0.062
	-0.231	-0.229	-0.227	-0.225	-0.224	-0.223
C(10)	-0.476	-0.478	-0.478	-0.479	-0.479	-0.479
	-0.374	-0.378	-0.382	-0.384	-0.387	-0.388
S(1)	0.283	0.286	0.288	0.291	0.295	0.296
	0.407	0.41	0.413	0.416	0.421	0.422
S(2)	0.283	0.281	0.278	0.275	0.271	0.266
	0.407	0.404	0.401	0.397	0.393	0.388
S(3)	0.116	0.124	0.132	0.14	0.152	0.129
	-0.084	-0.083	-0.082	-0.081	-0.081	-0.112
S(4)	0.116	0.108	0.097	0.087	0.075	0.063
	-0.084	-0.086	-0.089	-0.092	-0.096	-0.098
Au(2)	-0.037	-0.057	0.005	-0.105	-0.138	-0.182
	0.215	0.192	0.263	0.135	0.096	0.045
Au(1)	-0.037	-0.016	0.272	0.026	0.051	0.122
	0.215	0.239	0.251	0.287	0.316	0.391
H(2)	0.267	0.27	0.272	0.275	0.276	0.276
	0.248	0.249	0.251	0.253	0.255	0.256
H(3)	0.267	0.266	0.266	0.265	0.265	0.265
	0.242	0.241	0.241	0.24	0.24	0.241
H(9)	0.267	0.265	0.263	0.261	0.259	0.257
	0.248	0.246	0.245	0.243	0.242	0.241
H(8)	0.267	0.268	0.27	0.271	0.272	0.273
	0.242	0.243	0.243	0.244	0.245	0.246

4.1 Molecular orbital analysis

The electron transport characteristics [21] was well established from energy gap between the highest occupied molecular orbital (HOMO) and lowest unoccupied molecular orbital (LUMO). Thus it is essential to inspect the differences in HOMO-LUMO gap and molecular orbital energy levels for the different potential.

Figure. 7 shows the molecular orbital for the zero and higher levels of applied electric field for TET molecular wire. The applied EF moderately focuses the frontier orbitals of the system, which are differing to each other and are exceedingly symmetric when the direction of the field is inverted. The HLG decreases from 1.95 to 1.31 eV. The density of states (DOS) for the zero and non-zero bias (0.26 V \AA^{-1}) was depicted in the Fig 8, in which the green solid lines specify the HOMO and the blue shows the LUMO; the decrease of HLG is also shown.

EF (V \AA^{-1})	HOMO	
0.00		
	Positive field	Negative field
0.05		
0.10		
0.18		
0.21		
0.26		
EF (V \AA^{-1})	LUMO	

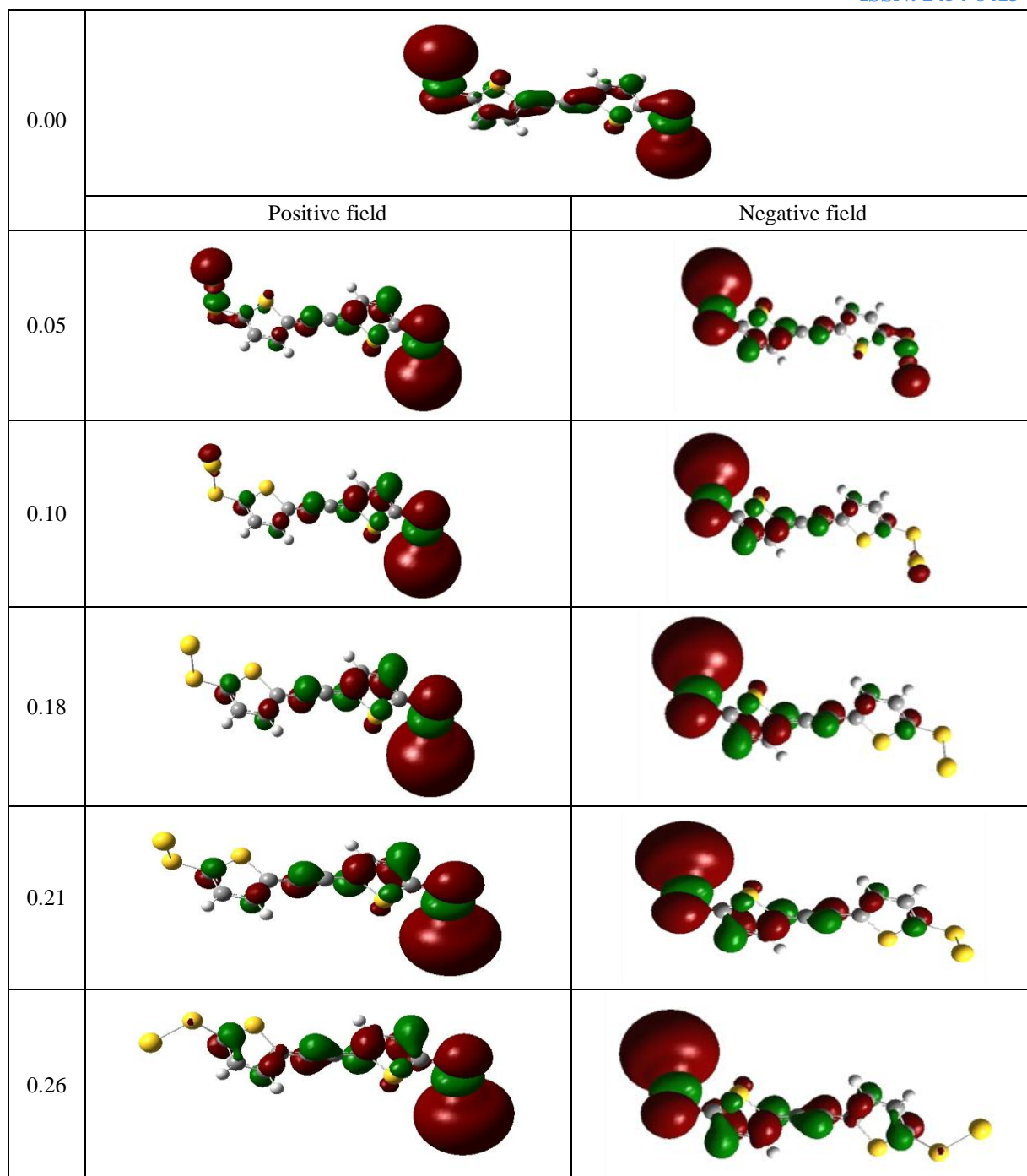


Figure. 7 Isosurface representation of molecular orbitals of Au and S substituted [(2R)-5-[2-[(2S)-5-aurosulfanyltetrahydrothiophen-2-yl]ethyl]tetrahydrothiophen-2-yl]sulfanylgold molecule for different potential.

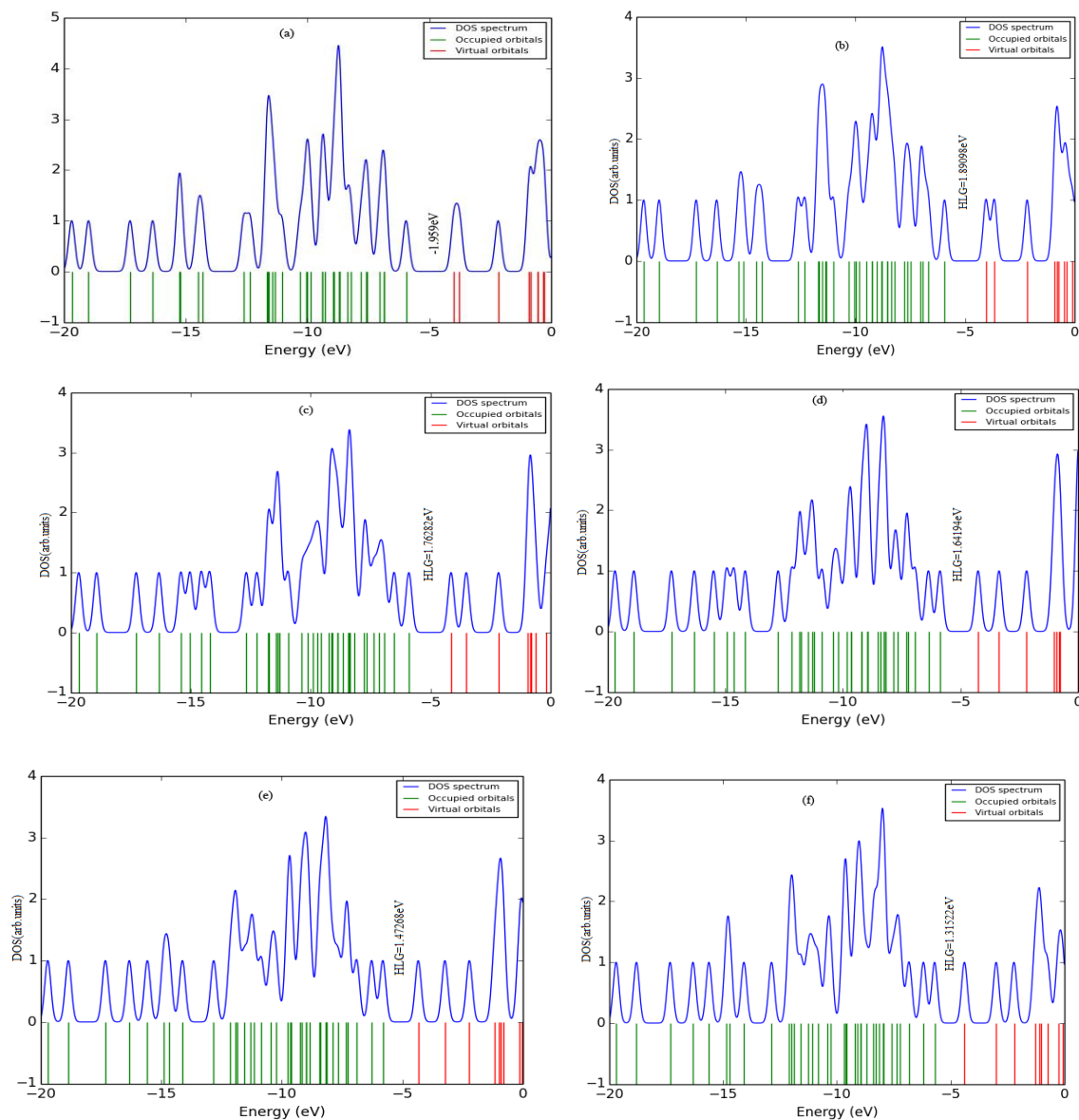


Figure. 8 DOS of Au and S substituted [(2R)-5-[2-[(2S)-5-aurosulfanyl]tetrahydrothiophen-2-yl]ethyl]tetrahydrothiophen-2-yl]sulfanylgold molecule for the different potential.

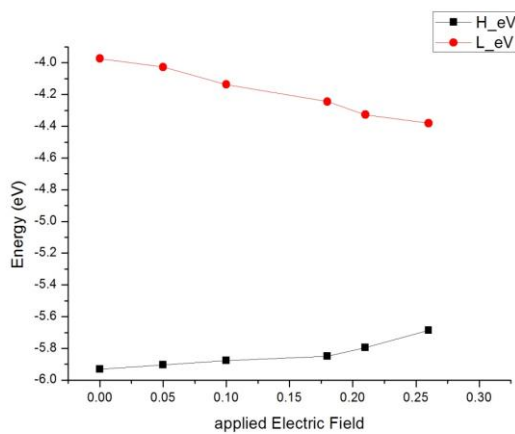


Figure. 9 Energy level diagram showing the HLG for the zero and various applied electric fields.

Markedly, the existence of Au atoms in the molecule at the terminal region widens the DOS peaks. The HOMO-LUMO gap is 2.0 eV for the zero electric field, and approaches to 1.31 eV when the applied electric field is increased from 0 to 0.26 eV. Apparently, the substantial drop of HLG may lead to high current conduction through the molecule, this shows that gold substituted TET molecule may behave as an effective molecular nanowire. The energy levels of the TET molecular wire for various applied electric fields were depicted in figure 9.

4.2 Molecular Electrostatic potential

The three-dimensional isosurface picture of electrostatic potential [22] of Au-S substituted TET wire was displayed in figure 10. As expected, the high negative potential (red) was mounted over the Au-S bond, which reflects the contrasting influences from the nuclei and the electrons.

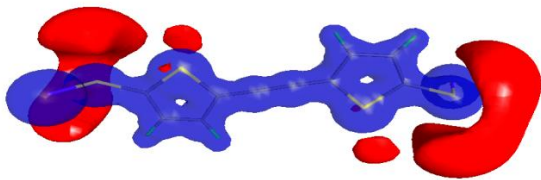
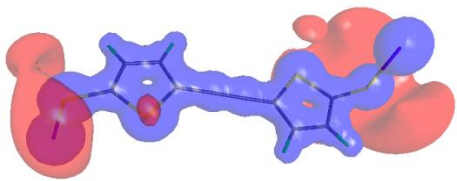
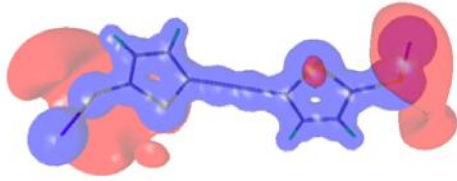
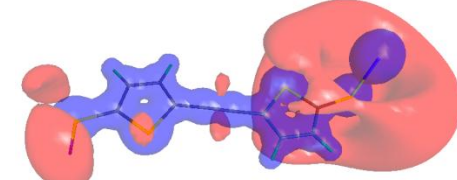
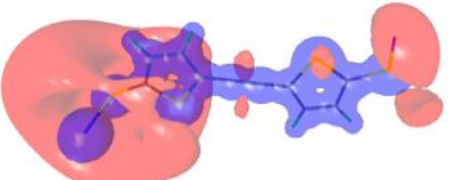
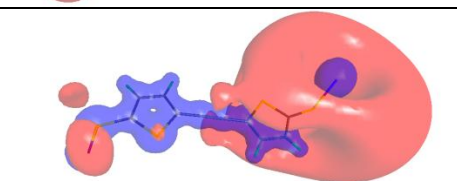
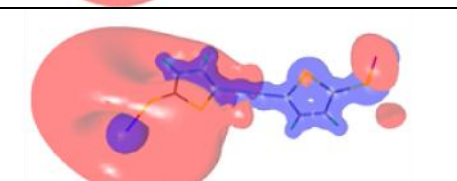
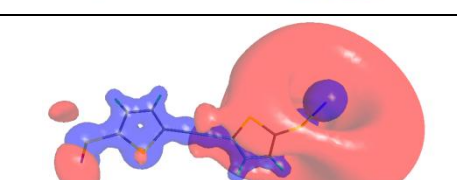
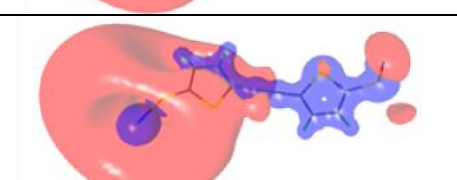
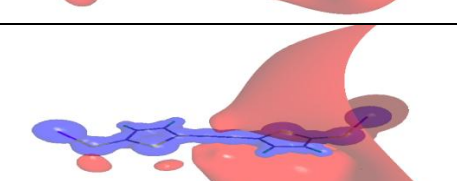
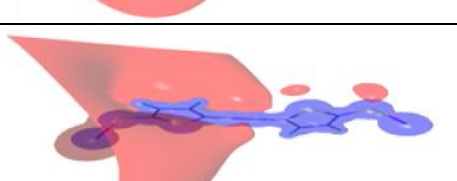
EF ($\text{V}\text{\AA}^{-1}$)	Electrostatic Potential	
0.00		
	Positive field	Negative field
0.05		
0.10		
0.18		
0.21		
0.26		

Figure.10 Molecular electrostatic potential of the molecule for the zero and various applied EFs. Blue: positive potential ($0.5 \text{ e}\text{\AA}^{-1}$), Red: negative potential ($-0.04 \text{ e}\text{\AA}^{-1}$). zero bias, the negative ESP is concentrated around the S-atoms, which are present at either ends of the molecule, and the rest of the molecule carries positive ESP.

When the positive electric field is increased from 0 to 0.26 eV, in the left end the negative electrostatic potential was found to be decreased at each step and it is much weaker at the maximum electric field, 0.26 eV. At the right edge, the negative electrostatic potential increased and dispersed across the R-end of the TET molecule. At the maximum electric field, 0.26 $\text{V}\text{\AA}^{-1}$, the negative electrostatic potential is completely covered over the right end terminal of the molecule; which depicts that migration of negative charge from left to right when the field increases. Conversely the negative charges were moved from right to left end of the molecule when the field is applied in the reverse manner.

4.3 Dipole moment

The external applied electric field polarizes the TET molecule, which results to modify the dipole moment of the molecule. Therefore it is vital to determine the dipole moment of the molecule for applied electric field. Kirtman et al., [23] reported the linear relationship between dipole moment and applied electric field. Conversely, this linear behaviour no longer persists beyond a specific applied electric field.

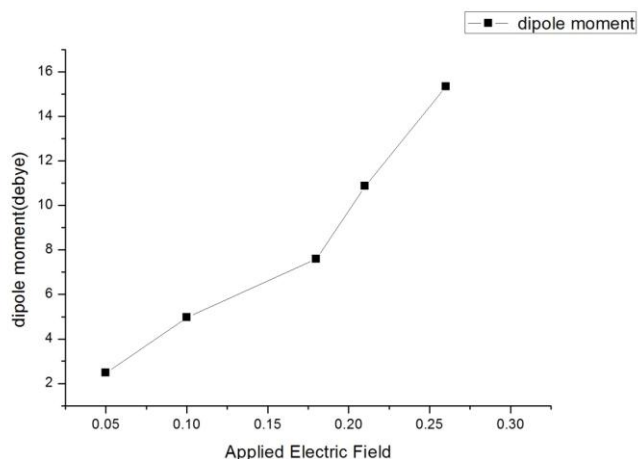


Figure. 11 Molecular dipole moment of the molecule for the zero and various applied EFs

The molecular dipole moment (μ) predicted at 0.05 eV is 2.47 debye, and when the electric field is increased further, this variation is found to be linear. At the maximum electric field, 0.26 eV, the TET molecule is found to be highly polarized with the dipole moment value, 15.33 debye. Because of the application of electric field along x-direction, the variation of dipole moment along x component is maximum μ_x , when compared with y and z components.

4.4 I–V Relation

The current–voltage curve commonly used to calculate the elementary factors of electronic devices [24]. The Landauer formula [25] has been established to determine the I-V characteristics. The voltage, V has been calculated from the equation $V = EL$, L is the length of the molecule. From Ohm's law, $I = V/R$ [26], the current passing was computed for each applied electric potential. Using these factors, the I–V characteristics of the TET molecule has been investigated. I–V curve of TET molecule for the applied electric fields was shown in the figure 12. As the applied electric field increases, the current also increases progressively presenting the nonlinear performance of the molecule. Since TET is symmetric, the curve is also nearly symmetric for positive and negative directions of the applied electric field.

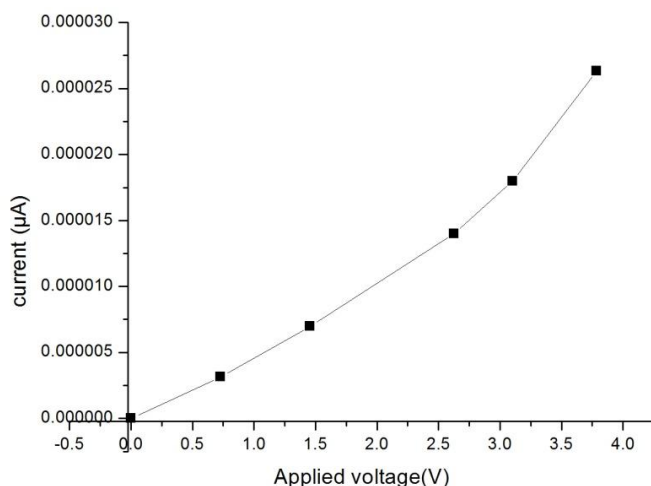


Figure.12 I–V Characteristics of TET molecule for different potential.

5. CONCLUSION

The geometry confirmation, topological bond properties and the electrical conductivity of gold and sulphur substituted TET molecular wire has been premeditated from the QTAIM theory via high level quantum chemical calculations for 0 to ± 0.26 eV applied electric fields. The bond distances of terminal S–C bond distance is smaller than the S-C bond length in the thiophene ring. When the applied electric field is increased from 0 eV, the Au–S bond distance at the right terminal is faintly longer than the left end; this variation is resulted from the gold atom at the left end which practices stronger electric field when compared with at the right end. The analysis of bond topology discloses that the deviation in electron density $\rho_{\text{bcp}}(r)$ and $\nabla^2 \rho_{\text{bcp}}(r)$ at the bond critical points of all the bonds for zero and the higher electric fields. The hybridization of molecular levels widens the density of states and the homo-lumo gap is decreased from 1.96 to 1.31 eV, which resulted in high electrical conductance through the TET molecule. The current-voltage curve seems very symmetric for the current flow in both directions through the molecule and it obviously shows the presence of nonlinear behavior of molecular wire. The applied electric field polarizes the TET molecule; as a result the dipole moment of the molecule rises from 2.47 to 15.33 D. Overall, the terminal groups of the TET molecules are responding very well towards the applied electric field.

REFERENCES

- [1]. Zade, SS & Bendikov, M (2006) From Oligomers to Polymer: Convergence in the HOMO–LUMO Gaps of Conjugated Oligomers. *Organic Letters*, 8(23), 5243-5246.
- [2]. Curtis, MD, Cao, J & Kampf JW (2004) Solid-State Packing of Conjugated Oligomers: From π -Stacks to the Herringbone Structure. *J Amer Chem Soc*, 126(13), 4318-4328.
- [3]. Bader, RFW (1991) A quantum theory of molecular structure and its applications. *Chem Rev*, 91(5), 893-928.
- [4]. Bagayoko, D (2014) Understanding density functional theory (DFT) and completing it in practice. *AIP Advances*, 4(12), 127104.
- [5]. Frisch, MJ, Trucks, GW, Schlegel, HB, Scuseria, GE, Robb, MA, Cheeseman, JA, Scalmani, G, Barone, V, Petersson, GA, Nakatsuji, H, Li, X, Caricato, M, Marenich, AV, Bloino, J, Janesko, BG, Gomperts, R, Mennucci, B, Hratchian, HP, Ortiz, JV, Izmaylov, AF, Sonnenberg, JL, Williams, F, Ding, Lipparini, F, Egidi, F, Goings, J, Peng, B, Petrone, A, Henderson, T, Ranasinghe, D, Zakrzewski, VG, Gao, J, Rega, N, Zheng, G, Liang, W, Hada, M, Ehara, M, Toyota, K, Fukuda, R, Hasegawa, J, Ishida, M, Nakajima, T, Honda, Y, Kitao, O, Nakai, H, Vreven, T, Throssell, K, Montgomery Jr., JA, Peralta, JE, Ogliaro, F, Bearpark, MJ, Heyd, JJ, Brothers, EN, Kudin, KN, Staroverov, VN, Keith, TA, Kobayashi, R, Normand, J, Raghavachari, K, Rendell, AP, Burant, JC, Iyengar, SS, Tomasi, J, Cossi, M, Millam, JM, Klene, M, Adamo, C, Cammi, R, Ochterski, JW, Martin, RL, Morokuma, K, Farkas, O, Foresman, JB & Fox JD, Gaussian 16 Rev. B.01. 2016: Wallingford, CT.
- [6]. Lee, C, Yang, W & Parr, RG (1988) Development of the Colle-Salvetti correlation-energy formula into a functional of the electron density. *Phy Rev B*, 37(2), 785-789.
- [7]. Wadt, WR & Hay PJ (1985) *Ab initio* effective core potentials for molecular calculations potentials for main group elements Na to Bi. *The Journal of Chemical Physics*, 82(1), 284-298.
- [8]. Cheeseman, J, Keith, TA, & Bader, RFW (1992) *AIMPAC Program Package*, McMaster University Hamilton, Ontario.
- [9]. Volkov, A, Koritsanszky, T, Chodkiewicz, M & King Harry, F (2008) On the basis- set dependence of local and integrated electron density properties: Application of a new computer program for quantum- chemical density analysis. *Jour of Comp Chem*, 30(9), 1379-1391.
- [10]. Dennington, R., Keith, TA & Millam, JM (2016) GaussView Version 6. Wallingford, CT.
- [11]. Koritsanszky, T, Macchi, P, Gatti, C, Farrugia, L, Mallison, PR, Volkov, A & Richter, T, (2006) XD2006- A computer program package for multipole refinement and analysis of charge densities from diffraction data. .
- [12]. O'Boyle Noel, M, Tenderholt Adam, L & Langner Karol, M (2007) cclib: A library for package independent computational chemistry algorithms. *Jour of Comp Chem*, 29(5), 839-845.
- [13]. Burgi, T, (2015) Properties of the gold-sulphur interface: from self-assembled monolayers to clusters. *Nanoscale*, 7(38), 15553-15567.
- [14]. Tachibana, M, Yoshizawa, K, Ogawa, A, Fujimoto, H & Hoffmann, R, (2002) Sulfur–Gold Orbital Interactions which Determine the Structure of Alkanethiolate/Au(111) Self-Assembled Monolayer Systems. *Jour of Phy Chem B*, 106(49), 12727-12736.
- [15]. Bader, R, (1994) *Atoms in Molecules: A Quantum Theory* (International Series of Monographs on Chemistry). Clarendon Press.
- [16]. Silva Lopez, C, & de Lera AR, (2011) Bond Ellipticity as a Measure of Electron Delocalization in Structure and Reactivity. *Curr Orga Chem*, 15(20), 3576-3593.
- [17]. Bader, RFW, & Preston, HJT, (1969) the kinetic energy of molecular charge distributions and molecular stability. *Inter Jour of Quant Chemi*, 3(3), 327-347.
- [18]. Gillespie, RJ, (2001) Electron Densities, Atomic Charges, and Ionic, Covalent, and Polar Bonds. *Journal of Chemical Education*, 78(12), 1688
- [19]. Saha, S, Roy Ram, K, & Ayers Paul, W (2008) Are the Hirshfeld and Mulliken population analysis schemes consistent with chemical intuition?, *Inter Jour Quant Chem*, 109(9), 1790-1806.
- [20]. Reed, AE, Weinstock, RB & Weinhold, F (1985) Natural population analysis. *Jour of Chem Phy*, 83(2), 735-746.
- [21]. Hu, P, Du, K, Wei, F, Jiang, H & Kloc, C (2016) Crystal Growth, HOMO–LUMO Engineering, and Charge Transfer Degree in Perylene-FxTCNQ (x = 1, 2, 4) Organic Charge Transfer Binary Compounds. *Crystal Growth & Design*, 16(5), 3019-3027.
- [22]. Politzer, P, Laurence, PR, & Jayasuriya, K (1985) Molecular electrostatic potentials: an effective tool for the elucidation of biochemical phenomena. *Environmental Health Perspectives*, 61, 191-202.
- [23]. Kirtman, B, Bonness, S, Ramirez-Solis, A, Champagne, B, Matsumoto, H, & Sekino, H (2008) Calculation of electric dipole (hyper) polarizabilities by long-range-correction scheme in density

- functional theory: A systematic assessment for polydiacetylene and polybutatriene oligomers. *Jour of Chem Phy*, 128(11), 114108.
- [24]. Darancet, P, Widawsky, JR, Choi, HJ, Venkataraman, L & Neaton, JB (2012) Quantitative Current–Voltage Characteristics in Molecular Junctions from First Principles. *Nano Letters*, 12(12), 6250-6254.
- [25]. Landauer, R, (2000) Spatial variation of currents and fields due to localized scatterers in metallic conduction. *IBM Journal of Research and Development*, 44(1), 251-260.
- [26]. Chapter 2 - Electrochemical and Thermodynamic Fundamentals, in *Membrane Science and Technology*, H. Strathmann, Editor. 2004, Elsevier. p. 23-88.